

Observation of B Meson Decays to ωK^* and Improved Measurements for $\omega\rho$ and ωf_0

B. Aubert,¹ Y. Karyotakis,¹ J. P. Lees,¹ V. Poireau,¹ E. Prencipe,¹ X. Prudent,¹ V. Tisserand,¹ J. Garra Tico,² E. Grauges,² L. Lopez^{ab,3}, A. Palano^{ab,3}, M. Pappagallo^{ab,3}, G. Eigen,⁴ B. Stugu,⁴ L. Sun,⁴ M. Battaglia,⁵ D. N. Brown,⁵ L. T. Kerth,⁵ Yu. G. Kolomensky,⁵ G. Lynch,⁵ I. L. Osipenkov,⁵ K. Tackmann,⁵ T. Tanabe,⁵ C. M. Hawkes,⁶ N. Soni,⁶ A. T. Watson,⁶ H. Koch,⁷ T. Schroeder,⁷ D. J. Asgeirsson,⁸ B. G. Fulsom,⁸ C. Hearty,⁸ T. S. Mattison,⁸ J. A. McKenna,⁸ M. Barrett,⁹ A. Khan,⁹ A. Randle-Conde,⁹ V. E. Blinov,¹⁰ A. D. Bukin,^{10,*} A. R. Buzykaev,¹⁰ V. P. Druzhinin,¹⁰ V. B. Golubev,¹⁰ A. P. Onuchin,¹⁰ S. I. Serednyakov,¹⁰ Yu. I. Skovpen,¹⁰ E. P. Solodov,¹⁰ K. Yu. Todyshev,¹⁰ M. Bondioli,¹¹ S. Curry,¹¹ I. Eschrich,¹¹ D. Kirkby,¹¹ A. J. Lankford,¹¹ P. Lund,¹¹ M. Mandelkern,¹¹ E. C. Martin,¹¹ D. P. Stoker,¹¹ S. Abachi,¹² C. Buchanan,¹² H. Atmacan,¹³ J. W. Gary,¹³ F. Liu,¹³ O. Long,¹³ G. M. Vitug,¹³ Z. Yasin,¹³ L. Zhang,¹³ V. Sharma,¹⁴ C. Campagnari,¹⁵ T. M. Hong,¹⁵ D. Kovalskyi,¹⁵ M. A. Mazur,¹⁵ J. D. Richman,¹⁵ T. W. Beck,¹⁶ A. M. Eisner,¹⁶ C. A. Heusch,¹⁶ J. Kroseberg,¹⁶ W. S. Lockman,¹⁶ A. J. Martinez,¹⁶ T. Schalk,¹⁶ B. A. Schumm,¹⁶ A. Seiden,¹⁶ L. O. Winstrom,¹⁶ C. H. Cheng,¹⁷ D. A. Doll,¹⁷ B. Echenard,¹⁷ F. Fang,¹⁷ D. G. Hitlin,¹⁷ I. Narsky,¹⁷ T. Piatenko,¹⁷ F. C. Porter,¹⁷ R. Andreassen,¹⁸ G. Mancinelli,¹⁸ B. T. Meadows,¹⁸ K. Mishra,¹⁸ M. D. Sokoloff,¹⁸ P. C. Bloom,¹⁹ W. T. Ford,¹⁹ A. Gaz,¹⁹ J. D. Gilman,¹⁹ J. F. Hirschauer,¹⁹ M. Nagel,¹⁹ U. Nauenberg,¹⁹ J. G. Smith,¹⁹ D. M. Rodriguez,¹⁹ E. W. Thomas,¹⁹ E. W. Tomassini,¹⁹ S. R. Wagner,¹⁹ R. Ayad,^{20,†} A. Soffer,^{20,‡} W. H. Toki,²⁰ R. J. Wilson,²⁰ E. Feltresi,²¹ A. Hauke,²¹ H. Jasper,²¹ M. Karbach,²¹ J. Merkel,²¹ A. Petzold,²¹ B. Spaan,²¹ K. Wacker,²¹ M. J. Kobel,²² R. Nogowski,²² K. R. Schubert,²² R. Schwierz,²² A. Volk,²² D. Bernard,²³ G. R. Bonneaud,²³ E. Latour,²³ M. Verderi,²³ P. J. Clark,²⁴ S. Playfer,²⁴ J. E. Watson,²⁴ M. Andreotti^{ab,25}, D. Bettoni^{a,25}, C. Bozzi^{a,25}, R. Calabrese^{ab,25}, A. Cecchi^{ab,25}, G. Cibinetto^{ab,25}, P. Franchini^{ab,25}, E. Luppi^{ab,25}, M. Negrini^{ab,25}, A. Petrella^{ab,25}, L. Piemontese^{a,25}, V. Santoro^{ab,25}, R. Baldini-Ferrolì,²⁶ A. Calcaterra,²⁶ R. de Sangro,²⁶ G. Finocchiaro,²⁶ S. Pacetti,²⁶ P. Patteri,²⁶ I. M. Peruzzi,^{26,§} M. Piccolo,²⁶ M. Rama,²⁶ A. Zallo,²⁶ R. Contri^{ab,27}, E. Guido,²⁷ M. Lo Vetere^{ab,27}, M. R. Monge^{ab,27}, S. Passaggio^{a,27}, C. Patrignani^{ab,27}, E. Robutti^{a,27}, S. Tosi^{ab,27}, K. S. Chaisanguanthum,²⁸ M. Morii,²⁸ A. Adametz,²⁹ J. Marks,²⁹ S. Schenk,²⁹ U. Uwer,²⁹ F. U. Bernlochner,³⁰ V. Klose,³⁰ H. M. Lacker,³⁰ D. J. Bard,³¹ P. D. Dauncey,³¹ M. Tibbetts,³¹ P. K. Behera,³² X. Chai,³² M. J. Charles,³² U. Mallik,³² J. Cochran,³³ H. B. Crawley,³³ L. Dong,³³ W. T. Meyer,³³ S. Prell,³³ E. I. Rosenberg,³³ A. E. Rubin,³³ Y. Y. Gao,³⁴ A. V. Gritsan,³⁴ Z. J. Guo,³⁴ N. Arnaud,³⁵ J. Béquilleux,³⁵ A. D’Orazio,³⁵ M. Davier,³⁵ J. Firmino da Costa,³⁵ G. Grosdidier,³⁵ F. Le Diberder,³⁵ V. Lepeltier,³⁵ A. M. Lutz,³⁵ S. Pruvot,³⁵ P. Roudeau,³⁵ M. H. Schune,³⁵ J. Serrano,³⁵ V. Sordini,^{35,¶} A. Stocchi,³⁵ G. Wormser,³⁵ D. J. Lange,³⁶ D. M. Wright,³⁶ I. Bingham,³⁷ J. P. Burke,³⁷ C. A. Chavez,³⁷ J. R. Fry,³⁷ E. Gabathuler,³⁷ R. Gamet,³⁷ D. E. Hutchcroft,³⁷ D. J. Payne,³⁷ C. Touramanis,³⁷ A. J. Bevan,³⁸ C. K. Clarke,³⁸ F. Di Lodovico,³⁸ R. Sacco,³⁸ M. Sigamani,³⁸ G. Cowan,³⁹ S. Paramesvaran,³⁹ A. C. Wren,³⁹ D. N. Brown,⁴⁰ C. L. Davis,⁴⁰ A. G. Denig,⁴¹ M. Fritsch,⁴¹ W. Gradl,⁴¹ A. Hafner,⁴¹ K. E. Alwyn,⁴² D. Bailey,⁴² R. J. Barlow,⁴² G. Jackson,⁴² G. D. Lafferty,⁴² T. J. West,⁴² J. I. Yi,⁴² J. Anderson,⁴³ C. Chen,⁴³ A. Jawahery,⁴³ D. A. Roberts,⁴³ G. Simi,⁴³ J. M. Tuggle,⁴³ C. Dallapiccola,⁴⁴ E. Salvati,⁴⁴ S. Saremi,⁴⁴ R. Cowan,⁴⁵ D. Dujmic,⁴⁵ P. H. Fisher,⁴⁵ S. W. Henderson,⁴⁵ G. Sciolla,⁴⁵ M. Spitznagel,⁴⁵ R. K. Yamamoto,⁴⁵ M. Zhao,⁴⁵ P. M. Patel,⁴⁶ S. H. Robertson,⁴⁶ M. Schram,⁴⁶ A. Lazzaro^{ab,47}, V. Lombardo^{a,47}, F. Palombo^{ab,47}, S. Stracka,⁴⁷ J. M. Bauer,⁴⁸ L. Cremaldi,⁴⁸ R. Godang,^{48,**} R. Kroeger,⁴⁸ D. J. Summers,⁴⁸ H. W. Zhao,⁴⁸ M. Simard,⁴⁹ P. Taras,⁴⁹ H. Nicholson,⁵⁰ G. De Nardo^{ab,51}, L. Lista^{a,51}, D. Monorchio^{ab,51}, G. Onorato^{ab,51}, C. Sciacca^{ab,51}, G. Raven,⁵² H. L. Snoek,⁵² C. P. Jessop,⁵³ K. J. Knoepfel,⁵³ J. M. LoSecco,⁵³ W. F. Wang,⁵³ L. A. Corwin,⁵⁴ K. Honscheid,⁵⁴ H. Kagan,⁵⁴ R. Kass,⁵⁴ J. P. Morris,⁵⁴ A. M. Rahimi,⁵⁴ J. J. Regensburger,⁵⁴ S. J. Sekula,⁵⁴ Q. K. Wong,⁵⁴ N. L. Blount,⁵⁵ J. Brau,⁵⁵ R. Frey,⁵⁵ O. Igonkina,⁵⁵ J. A. Kolb,⁵⁵ M. Lu,⁵⁵ R. Rahmat,⁵⁵ N. B. Sinev,⁵⁵ D. Strom,⁵⁵ J. Strube,⁵⁵ E. Torrence,⁵⁵ G. Castelli^{ab,56}, N. Gagliardi^{ab,56}, M. Margoni^{ab,56}, M. Morandin^{a,56}, M. Posocco^{a,56}, M. Rotondo^{a,56}, F. Simonetto^{ab,56}, R. Stroili^{ab,56}, C. Voci^{ab,56}, P. del Amo Sanchez,⁵⁷ E. Ben-Haim,⁵⁷ H. Briand,⁵⁷ J. Chauveau,⁵⁷ O. Hamon,⁵⁷ Ph. Leruste,⁵⁷ J. Ocariz,⁵⁷ A. Perez,⁵⁷ J. Prendki,⁵⁷ S. Sitt,⁵⁷ L. Gladney,⁵⁸ M. Biasini^{ab,59}, E. Manoni^{ab,59}, C. Angelini^{ab,60}, G. Batignani^{ab,60}, S. Bettarini^{ab,60}, G. Calderini^{ab,60,††}, M. Carpinelli^{ab,60,‡‡}

A. Cervelli^{ab,60} F. Forti^{ab,60} M. A. Giorgi^{ab,60} A. Lusiani^{ac,60} G. Marchiori^{ab,60} M. Morganti^{ab,60} N. Neri^{ab,60}
 E. Paoloni^{ab,60} G. Rizzo^{ab,60} J. J. Walsh^{a,60} D. Lopes Pegna,⁶¹ C. Lu,⁶¹ J. Olsen,⁶¹ A. J. S. Smith,⁶¹
 A. V. Telnov,⁶¹ F. Anulli^{a,62} E. Baracchini^{ab,62} G. Cavoto^{a,62} R. Faccini^{ab,62} F. Ferrarotto^{a,62} F. Ferroni^{ab,62}
 M. Gaspero^{ab,62} P. D. Jackson^{a,62} L. Li Gioi^{a,62} M. A. Mazzoni^{a,62} S. Morganti^{a,62} G. Piredda^{a,62} F. Renga^{ab,62}
 C. Voena^{a,62} M. Ebert,⁶³ T. Hartmann,⁶³ H. Schröder,⁶³ R. Waldi,⁶³ T. Adye,⁶⁴ B. Franek,⁶⁴ E. O. Olaiya,⁶⁴
 F. F. Wilson,⁶⁴ S. Emery,⁶⁵ L. Esteve,⁶⁵ G. Hamel de Monchenault,⁶⁵ W. Kozanecki,⁶⁵ G. Vasseur,⁶⁵ Ch. Yèche,⁶⁵
 M. Zito,⁶⁵ X. R. Chen,⁶⁶ H. Liu,⁶⁶ W. Park,⁶⁶ M. V. Purohit,⁶⁶ R. M. White,⁶⁶ J. R. Wilson,⁶⁶ M. T. Allen,⁶⁷
 D. Aston,⁶⁷ R. Bartoldus,⁶⁷ J. F. Benitez,⁶⁷ R. Cenci,⁶⁷ J. P. Coleman,⁶⁷ M. R. Convery,⁶⁷ J. C. Dingfelder,⁶⁷
 J. Dorfan,⁶⁷ G. P. Dubois-Felsmann,⁶⁷ W. Dunwoodie,⁶⁷ R. C. Field,⁶⁷ A. M. Gabareen,⁶⁷ M. T. Graham,⁶⁷
 P. Grenier,⁶⁷ C. Hast,⁶⁷ W. R. Innes,⁶⁷ J. Kaminski,⁶⁷ M. H. Kelsey,⁶⁷ H. Kim,⁶⁷ P. Kim,⁶⁷ M. L. Kocian,⁶⁷
 D. W. G. S. Leith,⁶⁷ S. Li,⁶⁷ B. Lindquist,⁶⁷ S. Luitz,⁶⁷ V. Luth,⁶⁷ H. L. Lynch,⁶⁷ D. B. MacFarlane,⁶⁷
 H. Marsiske,⁶⁷ R. Messner,^{67,*} D. R. Muller,⁶⁷ H. Neal,⁶⁷ S. Nelson,⁶⁷ C. P. O'Grady,⁶⁷ I. Ofte,⁶⁷ M. Perl,⁶⁷
 B. N. Ratcliff,⁶⁷ A. Roodman,⁶⁷ A. A. Salmikov,⁶⁷ R. H. Schindler,⁶⁷ J. Schwiening,⁶⁷ A. Snyder,⁶⁷ D. Su,⁶⁷
 M. K. Sullivan,⁶⁷ K. Suzuki,⁶⁷ S. K. Swain,⁶⁷ J. M. Thompson,⁶⁷ J. Va'vra,⁶⁷ A. P. Wagner,⁶⁷ M. Weaver,⁶⁷
 C. A. West,⁶⁷ W. J. Wisniewski,⁶⁷ M. Wittgen,⁶⁷ D. H. Wright,⁶⁷ H. W. Wulsin,⁶⁷ A. K. Yarritu,⁶⁷
 K. Yi,⁶⁷ C. C. Young,⁶⁷ V. Ziegler,⁶⁷ P. R. Burchat,⁶⁸ A. J. Edwards,⁶⁸ T. S. Miyashita,⁶⁸ S. Ahmed,⁶⁹
 M. S. Alam,⁶⁹ J. A. Ernst,⁶⁹ B. Pan,⁶⁹ M. A. Saeed,⁶⁹ S. B. Zain,⁶⁹ S. M. Spanier,⁷⁰ B. J. Wogland,⁷⁰
 R. Eckmann,⁷¹ J. L. Ritchie,⁷¹ A. M. Ruland,⁷¹ C. J. Schilling,⁷¹ R. F. Schwitters,⁷¹ B. W. Drummond,⁷²
 J. M. Izen,⁷² X. C. Lou,⁷² F. Bianchi^{ab,73} D. Gamba^{ab,73} M. Pelliccioni^{ab,73} M. Bomben^{ab,74} L. Bosisio^{ab,74}
 C. Cartaro^{ab,74} G. Della Ricca^{ab,74} L. Lanceri^{ab,74} L. Vitale^{ab,74} V. Azzolini,⁷⁵ N. Lopez-March,⁷⁵
 F. Martinez-Vidal,⁷⁵ D. A. Milanes,⁷⁵ A. Oyanguren,⁷⁵ J. Albert,⁷⁶ Sw. Banerjee,⁷⁶ B. Bhuyan,⁷⁶ H. H. F. Choi,⁷⁶
 K. Hamano,⁷⁶ G. J. King,⁷⁶ R. Kowalewski,⁷⁶ M. J. Lewczuk,⁷⁶ I. M. Nugent,⁷⁶ J. M. Roney,⁷⁶ R. J. Sobie,⁷⁶
 T. J. Gershon,⁷⁷ P. F. Harrison,⁷⁷ J. Ilic,⁷⁷ T. E. Latham,⁷⁷ G. B. Mohanty,⁷⁷ E. M. T. Puccio,⁷⁷
 H. R. Band,⁷⁸ X. Chen,⁷⁸ S. Dasu,⁷⁸ K. T. Flood,⁷⁸ Y. Pan,⁷⁸ R. Prepost,⁷⁸ C. O. Vuosalo,⁷⁸ and S. L. Wu⁷⁸

(The BABAR Collaboration)

¹Laboratoire d'Annecy-le-Vieux de Physique des Particules (LAPP),

Universit de Savoie, CNRS/IN2P3, F-74941 Annecy-Le-Vieux, France

²Universitat de Barcelona, Facultat de Fisica, Departament ECM, E-08028 Barcelona, Spain

³INFN Sezione di Bari^a; Dipartimento di Fisica, Università di Bari^b, I-70126 Bari, Italy

⁴University of Bergen, Institute of Physics, N-5007 Bergen, Norway

⁵Lawrence Berkeley National Laboratory and University of California, Berkeley, California 94720, USA

⁶University of Birmingham, Birmingham, B15 2TT, United Kingdom

⁷Ruhr Universität Bochum, Institut für Experimentalphysik 1, D-44780 Bochum, Germany

⁸University of British Columbia, Vancouver, British Columbia, Canada V6T 1Z1

⁹Brunel University, Uxbridge, Middlesex UB8 3PH, United Kingdom

¹⁰Budker Institute of Nuclear Physics, Novosibirsk 630090, Russia

¹¹University of California at Irvine, Irvine, California 92697, USA

¹²University of California at Los Angeles, Los Angeles, California 90024, USA

¹³University of California at Riverside, Riverside, California 92521, USA

¹⁴University of California at San Diego, La Jolla, California 92093, USA

¹⁵University of California at Santa Barbara, Santa Barbara, California 93106, USA

¹⁶University of California at Santa Cruz, Institute for Particle Physics, Santa Cruz, California 95064, USA

¹⁷California Institute of Technology, Pasadena, California 91125, USA

¹⁸University of Cincinnati, Cincinnati, Ohio 45221, USA

¹⁹University of Colorado, Boulder, Colorado 80309, USA

²⁰Colorado State University, Fort Collins, Colorado 80523, USA

²¹Technische Universität Dortmund, Fakultät Physik, D-44221 Dortmund, Germany

²²Technische Universität Dresden, Institut für Kern- und Teilchenphysik, D-01062 Dresden, Germany

²³Laboratoire Leprince-Ringuet, CNRS/IN2P3, Ecole Polytechnique, F-91128 Palaiseau, France

²⁴University of Edinburgh, Edinburgh EH9 3JZ, United Kingdom

²⁵INFN Sezione di Ferrara^a; Dipartimento di Fisica, Università di Ferrara^b, I-44100 Ferrara, Italy

²⁶INFN Laboratori Nazionali di Frascati, I-00044 Frascati, Italy

²⁷INFN Sezione di Genova^a; Dipartimento di Fisica, Università di Genova^b, I-16146 Genova, Italy

²⁸Harvard University, Cambridge, Massachusetts 02138, USA

²⁹Universität Heidelberg, Physikalisches Institut, Philosophenweg 12, D-69120 Heidelberg, Germany

³⁰Humboldt-Universität zu Berlin, Institut für Physik, Newtonstr. 15, D-12489 Berlin, Germany

³¹Imperial College London, London, SW7 2AZ, United Kingdom

- ³² University of Iowa, Iowa City, Iowa 52242, USA
- ³³ Iowa State University, Ames, Iowa 50011-3160, USA
- ³⁴ Johns Hopkins University, Baltimore, Maryland 21218, USA
- ³⁵ Laboratoire de l'Accélérateur Linéaire, IN2P3/CNRS et Université Paris-Sud 11, Centre Scientifique d'Orsay, B. P. 34, F-91898 Orsay Cedex, France
- ³⁶ Lawrence Livermore National Laboratory, Livermore, California 94550, USA
- ³⁷ University of Liverpool, Liverpool L69 7ZE, United Kingdom
- ³⁸ Queen Mary, University of London, London, E1 4NS, United Kingdom
- ³⁹ University of London, Royal Holloway and Bedford New College, Egham, Surrey TW20 0EX, United Kingdom
- ⁴⁰ University of Louisville, Louisville, Kentucky 40292, USA
- ⁴¹ Johannes Gutenberg-Universität Mainz, Institut für Kernphysik, D-55099 Mainz, Germany
- ⁴² University of Manchester, Manchester M13 9PL, United Kingdom
- ⁴³ University of Maryland, College Park, Maryland 20742, USA
- ⁴⁴ University of Massachusetts, Amherst, Massachusetts 01003, USA
- ⁴⁵ Massachusetts Institute of Technology, Laboratory for Nuclear Science, Cambridge, Massachusetts 02139, USA
- ⁴⁶ McGill University, Montréal, Québec, Canada H3A 2T8
- ⁴⁷ INFN Sezione di Milano^a; Dipartimento di Fisica, Università di Milano^b, I-20133 Milano, Italy
- ⁴⁸ University of Mississippi, University, Mississippi 38677, USA
- ⁴⁹ Université de Montréal, Physique des Particules, Montréal, Québec, Canada H3C 3J7
- ⁵⁰ Mount Holyoke College, South Hadley, Massachusetts 01075, USA
- ⁵¹ INFN Sezione di Napoli^a; Dipartimento di Scienze Fisiche, Università di Napoli Federico II^b, I-80126 Napoli, Italy
- ⁵² NIKHEF, National Institute for Nuclear Physics and High Energy Physics, NL-1009 DB Amsterdam, The Netherlands
- ⁵³ University of Notre Dame, Notre Dame, Indiana 46556, USA
- ⁵⁴ Ohio State University, Columbus, Ohio 43210, USA
- ⁵⁵ University of Oregon, Eugene, Oregon 97403, USA
- ⁵⁶ INFN Sezione di Padova^a; Dipartimento di Fisica, Università di Padova^b, I-35131 Padova, Italy
- ⁵⁷ Laboratoire de Physique Nucléaire et de Hautes Energies, IN2P3/CNRS, Université Pierre et Marie Curie-Paris6, Université Denis Diderot-Paris7, F-75252 Paris, France
- ⁵⁸ University of Pennsylvania, Philadelphia, Pennsylvania 19104, USA
- ⁵⁹ INFN Sezione di Perugia^a; Dipartimento di Fisica, Università di Perugia^b, I-06100 Perugia, Italy
- ⁶⁰ INFN Sezione di Pisa^a; Dipartimento di Fisica, Università di Pisa^b; Scuola Normale Superiore di Pisa^c, I-56127 Pisa, Italy
- ⁶¹ Princeton University, Princeton, New Jersey 08544, USA
- ⁶² INFN Sezione di Roma^a; Dipartimento di Fisica, Università di Roma La Sapienza^b, I-00185 Roma, Italy
- ⁶³ Universität Rostock, D-18051 Rostock, Germany
- ⁶⁴ Rutherford Appleton Laboratory, Chilton, Didcot, Oxon, OX11 0QX, United Kingdom
- ⁶⁵ CEA, Irfu, SPP, Centre de Saclay, F-91191 Gif-sur-Yvette, France
- ⁶⁶ University of South Carolina, Columbia, South Carolina 29208, USA
- ⁶⁷ SLAC National Accelerator Laboratory, Stanford, CA 94309, USA
- ⁶⁸ Stanford University, Stanford, California 94305-4060, USA
- ⁶⁹ State University of New York, Albany, New York 12222, USA
- ⁷⁰ University of Tennessee, Knoxville, Tennessee 37996, USA
- ⁷¹ University of Texas at Austin, Austin, Texas 78712, USA
- ⁷² University of Texas at Dallas, Richardson, Texas 75083, USA
- ⁷³ INFN Sezione di Torino^a; Dipartimento di Fisica Sperimentale, Università di Torino^b, I-10125 Torino, Italy
- ⁷⁴ INFN Sezione di Trieste^a; Dipartimento di Fisica, Università di Trieste^b, I-34127 Trieste, Italy
- ⁷⁵ IFIC, Universitat de Valencia-CSIC, E-46071 Valencia, Spain
- ⁷⁶ University of Victoria, Victoria, British Columbia, Canada V8W 3P6
- ⁷⁷ Department of Physics, University of Warwick, Coventry CV4 7AL, United Kingdom
- ⁷⁸ University of Wisconsin, Madison, Wisconsin 53706, USA

(Dated: October 30, 2018)

We present measurements of B meson decays to the final states ωK^* , $\omega\rho$, and ωf_0 , where K^* indicates a spin 0, 1, or 2 strange meson. The data sample corresponds to 465×10^6 $B\bar{B}$ pairs collected with the BABAR detector at the PEP-II e^+e^- collider at SLAC. B meson decays involving vector-scalar, vector-vector, and vector-tensor final states are analyzed; the latter two shed new light on the polarization of these final states. We measure the branching fractions for nine of these decays; five are observed for the first time. For most decays we also measure the charge asymmetry and, where relevant, the longitudinal polarization f_L .

Studies of vector-vector (VV) final states in B decays resulted in the surprising observation that the longitudinal polarization fraction f_L in $B \rightarrow \phi K^*$ decays is ~ 0.5 , not ~ 1 [1]. The latter value is expected from simple helicity arguments and has been confirmed in the tree-dominated [2] $B \rightarrow \rho\rho$ decays [3] and $B^+ \rightarrow \omega\rho^+$ decays [4]. It appears that the $f_L \sim 1$ expectation is correct for tree-dominated decays but is not generally true for decays where $b \rightarrow s$ loop (penguin) amplitudes are dominant.

There have been numerous attempts to understand the polarization puzzle (small f_L) within the Standard Model (SM) [5], and many papers have suggested non-SM explanations [6]. The SM picture improved recently with the calculation of f_L for most charmless VV decays [2] with inclusion of non-factorizable effects and penguin annihilation amplitudes. Improved understanding of these effects can come from branching fraction and f_L measurements in decays such as $B \rightarrow \omega K^*$, which is related to $B \rightarrow \phi K^*$ via SU(3) symmetry [7]. Among these decays, there is evidence for only $B^0 \rightarrow \omega K^{*0}$ [4, 8]. Information on these and related charmless B decays can be used to provide constraints on the CKM angles α , β , and γ [9].

Further information on the polarization puzzle can come from measurements that include the tensor meson $K_2^*(1430)$. A measurement of the vector-tensor (VT) decay $B \rightarrow \phi K_2^*(1430)$ [10] finds a value of f_L inconsistent with 0.5 (but consistent with 1), so a measurement of the related decay $B \rightarrow \omega K_2^*(1430)$ would be interesting. The only theoretical predictions for these modes are from generalized factorization calculations [11]; the branching fraction predictions for the $B \rightarrow \omega K_2^*(1430)$ decays are $\sim (1 - 2) \times 10^{-6}$, but there are no predictions for f_L . There have been a variety of measurements for similar B decays that include the scalar meson $K_0^*(1430)$ [10, 12]. For the scalar-vector (SV) decays $B \rightarrow \omega K_0^*(1430)$, there are recent QCD factorization calculations [13] that predict branching fractions of about 10^{-6} .

We report measurements of B decays to the final states ωK^* , $\omega\rho$, and $\omega f_0(980)$, where K^* includes the spin 0, 1, and 2 states, $K_0^*(1430)$, $K^*(892)$, and $K_2^*(1430)$, respectively. While a complete angular analysis of the VV and VT decays would determine helicity amplitudes fully, because of the small signal samples we measure only f_L . Given our uniform azimuthal acceptance, we obtain, after integration, the angular distributions $d^2\Gamma/(d \cos \theta_1 d \cos \theta_2)$:

$$f_T \sin^2 \theta_1 \sin^2 \theta_2 + 4f_L \cos^2 \theta_1 \cos^2 \theta_2, \quad (1)$$

$$f_T \sin^2 \theta_1 \sin^2 \theta_2 \cos^2 \theta_2 + \frac{f_L}{3} \cos^2 \theta_1 (3 \cos^2 \theta_2 - 1)^2 \quad (2)$$

for the VV and VT [14] decays, respectively, where $f_T = 1 - f_L$ and θ_1 and θ_2 are the helicity angles in the V or T rest frame with respect to the boost axis from the B rest frame. For decays with significant signals, we also measure the direct CP -violating, time-integrated charge

TABLE I: Selection requirements on the invariant masses and helicity angles of B -daughter resonances. The helicity angle is unrestricted unless indicated otherwise.

State	inv. mass (MeV)	helicity angle
$K_{K^+\pi^-}^{*0}, K_{K_S^0\pi^+}^{*+}$	$750 < m_{K\pi} < 1550$	$-0.85 < \cos \theta < 1.0$
$K_{K^+\pi^0}^{*+}$	$750 < m_{K\pi} < 1550$	$-0.80 < \cos \theta < 1.0$
ρ^0/f_0	$470 < m_{\pi\pi} < 1070$	$-0.80 < \cos \theta < 0.80$
ρ^+	$470 < m_{\pi\pi} < 1070$	$-0.70 < \cos \theta < 0.80$
ω	$735 < m_{\pi\pi\pi} < 825$	
π^0	$120 < m_{\gamma\gamma} < 150$	
K_S^0	$488 < m_{\pi\pi} < 508$	

asymmetry $\mathcal{A}_{ch} \equiv (\Gamma^- - \Gamma^+)/(\Gamma^- + \Gamma^+)$, where the superscript on the Γ corresponds to the charge of the B^\pm meson or the charge of the kaon for B^0 decays.

The results presented here are obtained from data collected with the BABAR detector [15] at the PEP-II asymmetric-energy e^+e^- collider located at SLAC. An integrated luminosity of 424 fb^{-1} , corresponding to $465 \times 10^6 B\bar{B}$ pairs, was recorded at the $\Upsilon(4S)$ resonance, with e^+e^- center-of-mass (CM) energy $\sqrt{s} = 10.58 \text{ GeV}$.

Charged particles from the e^+e^- interactions are detected, and their momenta measured, by five layers of double-sided silicon microstrip detectors surrounded by a 40-layer drift chamber, both operating in the 1.5-T magnetic field of a superconducting solenoid. We identify photons and electrons using a CsI(Tl) electromagnetic calorimeter (EMC). Further charged particle identification (PID) is provided by the average energy loss (dE/dx) in the tracking devices and by an internally reflecting ring-imaging Cherenkov detector (DIRC) covering the central region.

We reconstruct B -daughter candidates through their decays $\rho^0 \rightarrow \pi^+\pi^-$, $f_0(980) \rightarrow \pi^+\pi^-$, $\rho^+ \rightarrow \pi^+\pi^0$, $K^{*0} \rightarrow K^+\pi^-$, $K^{*+} \rightarrow K^+\pi^0(K_{K^+\pi^0}^{*+})$, $K^{*+} \rightarrow K_S^0\pi^+(K_{K_S^0\pi^+}^{*+})$, $\omega \rightarrow \pi^+\pi^-\pi^0$, $\pi^0 \rightarrow \gamma\gamma$, and $K_S^0 \rightarrow \pi^+\pi^-$. Charge-conjugate decay modes are implied unless specifically stated. Table I lists the requirements on the invariant masses of these final states. For the ρ , K^* , and ω selections, these mass requirements include sidebands, as the mass values are treated as observables in the maximum-likelihood fit described below. For K_S^0 candidates we further require the three-dimensional flight distance from the primary vertex to be greater than three times its uncertainty. Daughters of ρ , K^* , and ω candidates are rejected if their DIRC, dE/dx , and EMC PID signatures are highly consistent with protons or electrons; kaons must have a kaon signature while the pions must not.

Table I also gives the restrictions on the K^* and ρ helicity angle θ imposed to avoid regions of large combinatorial background from low-momentum particles. To calculate θ we take the angle relative to a specified axis:

for ω , the normal to the decay plane; for ρ , the positively-charged daughter momentum; and for K^* , the daughter kaon momentum.

A B -meson candidate is characterized kinematically by the energy-substituted mass $m_{\text{ES}} \equiv \sqrt{(\frac{1}{2}s + \mathbf{p}_0 \cdot \mathbf{p}_B)^2 / E_0^{*2} - \mathbf{p}_B^2}$ and the energy difference $\Delta E \equiv E_B^* - \frac{1}{2}\sqrt{s}$, where (E_0, \mathbf{p}_0) and (E_B, \mathbf{p}_B) are four-momenta of the e^+e^- CM and the B candidate, respectively, s is the square of the CM energy, and the asterisk denotes the e^+e^- CM frame. Signal events peak at zero for ΔE , and at the B mass [16] for m_{ES} , with a resolution for ΔE (m_{ES}) of 30–45 MeV (3.0 MeV). We require $|\Delta E| \leq 0.2$ GeV and $5.25 \leq m_{\text{ES}} < 5.29$ GeV.

The angle θ_{T} between the thrust axis of the B candidate in the e^+e^- CM frame and that of the charged tracks and neutral clusters in the rest of the event is used to reject the dominant continuum $e^+e^- \rightarrow q\bar{q}$ ($q = u, d, s, c$) background events. The distribution of $|\cos\theta_{\text{T}}|$ is sharply peaked near 1.0 for combinations drawn from jet-like $q\bar{q}$ pairs, and is nearly uniform for the almost isotropic B -meson decays. We reduce the sample sizes to 30000–65000 events by requiring $|\cos\theta_{\text{T}}| < 0.7$ for the $\omega\rho/f_0$ modes and $|\cos\theta_{\text{T}}| < 0.8$ for the ωK^* modes. Further discrimination from continuum is obtained with a Fisher discriminant \mathcal{F} that combines four variables: the polar angles, with respect to the beam axis in the e^+e^- CM frame, of the B candidate momentum and of the B thrust axis; and the zeroth and second angular moments $L_{0,2}$ of the energy flow, excluding the B candidate, about the B thrust axis. The mean of \mathcal{F} is adjusted so that it is independent of the B -flavor tagging category [17]. The moments are defined by $L_j = \sum_i p_i \times |\cos\theta_i|^j$, where θ_i is the angle with respect to the B thrust axis of track or neutral cluster i and p_i is its momentum. The average number of B candidates found per selected event in data is in the range 1.1 to 1.3, depending on the final state. We choose the candidate with the highest value of the probability for the B vertex fit.

We obtain yields and values of f_L and \mathcal{A}_{ch} from extended unbinned maximum-likelihood (ML) fits with input observables ΔE , m_{ES} , \mathcal{F} , and, for the scalar, vector or tensor meson, the invariant mass and $\mathcal{H} = \cos\theta$. For each event i and hypothesis j (signal, $q\bar{q}$ background, $B\bar{B}$ background), we define the probability density function (PDF) with resulting likelihood \mathcal{L} :

$$\mathcal{P}_j^i = \mathcal{P}_j(m_{\text{ES}}^i) \mathcal{P}_j(\Delta E^i) \mathcal{P}_j(\mathcal{F}^i) \mathcal{P}_j(m_1^i, m_2^i, \mathcal{H}_1^i, \mathcal{H}_2^i), \quad (3)$$

$$\mathcal{L} = \frac{e^{-(\sum_j Y_j)}}{N!} \prod_{i=1}^N \sum_j Y_j \mathcal{P}_j^i, \quad (4)$$

where Y_j is the yield of events of hypothesis j , N is the number of events in the sample, and the subscript 1 (2) represents 3π ($K\pi$ or $\pi\pi$). There are as many as three signal categories and the PDFs for each are split into two components: correctly reconstructed events and those

where candidate particles are exchanged with a particle from the rest of the event. The latter component is called self crossfeed (SXF) and its fractions are fixed to the values found in Monte Carlo (MC), (15–35)%. We find correlations among the observables to be small for $q\bar{q}$ background.

From MC simulation [18] we form a sample of the most relevant charmless $B\bar{B}$ backgrounds (20–35 modes for each signal final state). We include a fixed yield (70–200 events, derived from MC with known or estimated branching fractions) for these in the fit described below. For $B^+ \rightarrow \omega\rho^+$ we also introduce a component for non-resonant $\omega\pi^+\pi^0$ background; for the other decays non-resonant backgrounds are smaller and are included in the charmless $B\bar{B}$ sample. The magnitude of the non-resonant component is fixed in each fit as determined from fits to regions of higher $\pi\pi$ or $K\pi$ mass. For the $\omega\rho$ modes, we also include a sample of $b \rightarrow c$ backgrounds; for the other modes, this component is not used since it is not clearly distinguishable from $q\bar{q}$ background.

Signal is also simulated with MC; for the $(K\pi)_0^*$ line shape, we use a LASS model [19, 20] which consists of the $K_0^*(1430)$ resonance together with an effective-range nonresonant component. For the $f_0(980)$, we use a Breit-Wigner shape with parameters taken from Ref. [21].

The PDF for resonances in the signal takes the form $\mathcal{P}_{1,\text{sig}}(m_1^i) \mathcal{P}_{2,\text{sig}}(m_2^i) \mathcal{Q}(\mathcal{H}_1^i, \mathcal{H}_2^i)$ with \mathcal{Q} given by Eq. 1 or 2, modified to account for detector acceptance. For $q\bar{q}$ background we use for each resonance independently $\mathcal{P}_{q\bar{q}}(m_k^i, \mathcal{H}_k^i) = \mathcal{P}_{q\bar{q}}(m_k^i) \mathcal{P}_{q\bar{q}}(\mathcal{H}_k^i)$, where $\mathcal{P}_{q\bar{q}}(m_k^i)$ is a sum of true resonance and combinatorial mass terms. The PDFs for $B\bar{B}$ background have a similar form.

For the signal, $B\bar{B}$ background, and nonresonant background components we determine the PDF parameters from simulation. We study large data control samples of $B^+ \rightarrow \bar{D}^0\pi^+$ and $B^+ \rightarrow \bar{D}^0\rho^+$ decays with $\bar{D}^0 \rightarrow K^+\pi^-\pi^0$ to check the simulated resolutions in ΔE and m_{ES} , and adjust the PDF parameters to account for small differences. For the continuum background we use $(m_{\text{ES}}, \Delta E)$ sideband data to obtain initial values of the parameters, and leave them free to vary in the ML fit.

The parameters that are allowed to vary in the fit include the signal and $q\bar{q}$ background yields, f_L (for all VV and VT modes except $B^0 \rightarrow \omega\rho^0$), continuum background PDF parameters, and, for $\omega\rho$, the $b \rightarrow c$ background yield. Since there is not a significant yield for $B^0 \rightarrow \omega\rho^0$, we fix f_L to a value that is consistent with *a priori* expectations [2] (see Table II). For all modes except $B^0 \rightarrow \omega\rho^0$ the signal and background charge asymmetries are free parameters in the fit.

To describe the PDFs, we use simple functions such as the sum of two Gaussian distributions for many signal components and the peaking parts of backgrounds, low-order polynomials to describe most background shapes, an asymmetric Gaussian for \mathcal{F} , and the function $x\sqrt{1-x^2} \exp[-\xi(1-x^2)]$ (with $x \equiv m_{\text{ES}}/E_B^*$) for the

TABLE II: Signal yield Y and its statistical uncertainty, bias Y_0 , detection efficiency ϵ , daughter branching fraction product $\prod \mathcal{B}_i$, significance S (with systematic uncertainties included), measured branching fraction \mathcal{B} with statistical and systematic errors, 90% C.L. upper limit (U.L.), measured or assumed f_L , and \mathcal{A}_{ch} . In the case of ωf_0 , the quoted branching fraction is a product with $\mathcal{B}(f_0 \rightarrow \pi\pi)$, which is not well known. $(K\pi)_0^*$ refers to the S-wave $K\pi$ system.

Mode	Y (events)	Y_0 (events)	ϵ (%)	$\prod \mathcal{B}_i$ (%)	S (σ)	\mathcal{B} (10^{-6})	\mathcal{B} U.L. (10^{-6})	f_L	\mathcal{A}_{ch}
ωK^{*0}	101 ± 25	8 ± 4	15.2	59.5	4.1	$2.2 \pm 0.6 \pm 0.2$	—	$0.72 \pm 0.14 \pm 0.02$	$0.45 \pm 0.25 \pm 0.02$
ωK^{*+}					2.5	$2.4 \pm 1.0 \pm 0.2$	7.4	$0.41 \pm 0.18 \pm 0.05$	$0.29 \pm 0.35 \pm 0.02$
$\omega K_{K^+\pi^0}^{*+}$	72 ± 24	3 ± 2	10.4	29.7	3.7	4.8 ± 1.7		0.37 ± 0.18	0.22 ± 0.33
$\omega K_{K_S^0\pi^+}^{*+}$	8 ± 16	0 ± 1	13.6	20.6	0.5	0.6 ± 1.2		0.5 fixed	—
$\omega(K\pi)_0^{*+}$	540 ± 47	49 ± 25	9.7	59.5	9.8	$18.4 \pm 1.8 \pm 1.7$	—	—	$-0.07 \pm 0.09 \pm 0.02$
$\omega(K\pi)_0^{*+}$					9.2	$27.5 \pm 3.0 \pm 2.6$	—	—	$-0.10 \pm 0.09 \pm 0.02$
$\omega(K^+\pi^0)_0^{*+}$	191 ± 36	18 ± 9	6.4	29.7	5.9	19.6 ± 4.1	—	—	-0.38 ± 0.19
$\omega(K_S^0\pi^+)_0^{*+}$	357 ± 39	34 ± 17	9.1	20.6	10.6	37.1 ± 4.5	—	—	-0.01 ± 0.10
$\omega K_2^*(1430)_0^0$	185 ± 32	19 ± 10	11.9	29.7	5.0	$10.1 \pm 2.0 \pm 1.1$	—	$0.45 \pm 0.12 \pm 0.02$	$-0.37 \pm 0.17 \pm 0.02$
$\omega K_2^*(1430)^+$					6.1	$21.5 \pm 3.6 \pm 2.4$	—	$0.56 \pm 0.10 \pm 0.04$	$0.14 \pm 0.15 \pm 0.02$
$\omega K_2^*(1430)_{K^+\pi^0}^+$	182 ± 30	6 ± 3	8.2	14.9	7.2	31.0 ± 5.2	—	0.52 ± 0.10	0.17 ± 0.16
$\omega K_2^*(1430)_{K_S^0\pi^+}^+$	64 ± 25	10 ± 5	10.1	10.3	2.4	11.2 ± 4.9	—	0.76 ± 0.26	-0.04 ± 0.35
$\omega\rho^0$	30^{+21}_{-18}	-3 ± 2	9.5	89.2	1.9	$0.8 \pm 0.5 \pm 0.2$	1.6	0.8 fixed	—
ωf_0	37^{+14}_{-12}	1 ± 1	14.4	59.5	4.5	$1.0 \pm 0.3 \pm 0.1$	1.5	—	—
$\omega\rho^+$	411 ± 43	27 ± 14	5.8	89.2	9.8	$15.9 \pm 1.6 \pm 1.4$	—	$0.90 \pm 0.05 \pm 0.03$	$-0.20 \pm 0.09 \pm 0.02$

m_{ES} background distributions. These are illustrated for $B^+ \rightarrow \omega\rho^+$ with projection plots of each fit variable in Figs. 1, 2d, and 3d. The parameters that determine the main features of the background PDF shapes are allowed to vary in the fit.

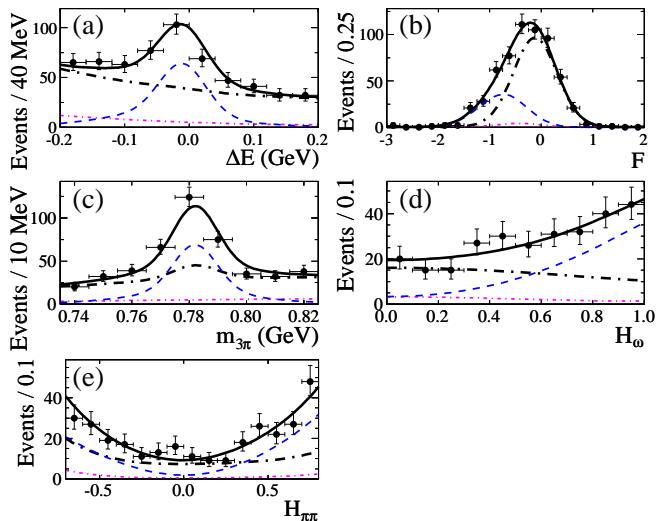


FIG. 1: Projections for $B^+ \rightarrow \omega\rho^+$: (a) ΔE , (b) \mathcal{F} , (c) $m_{3\pi}$, (d) \mathcal{H}_ω , and (e) $\mathcal{H}_{\pi\pi}$. Points with errors represent data and solid curves represent the full fit functions. Also shown are signal (blue dashed), $b \rightarrow c$ background (magenta dot-dashed), and total background (black long-dash-dotted). Charmless background and nonresonant background are too small to be seen. To suppress background, the plots are made with requirements on $\ln \mathcal{L}$ that have an efficiency for signal of (40-60)% depending on the plot.

We evaluate biases from our neglect of correlations among discriminating variables by fitting ensembles of simulated experiments. Each such experiment has the same number of events as the data for both background and signal; $q\bar{q}$ background events are generated from their PDFs while signal and $B\bar{B}$ background events are taken from fully simulated MC samples. Since events from the $B\bar{B}$ background samples are included in the ensembles, the bias includes the effect of these backgrounds.

We compute the branching fraction \mathcal{B} for each decay by subtracting the yield bias Y_0 from the measured yield, and dividing the result by the efficiency and the number of produced $B\bar{B}$ pairs. We assume that the branching fractions of the $\Upsilon(4S)$ to B^+B^- and $B^0\bar{B}^0$ are each equal to 50%. In Table II we show for each decay mode the measured \mathcal{B} , f_L , and \mathcal{A}_{ch} together with the quantities entering into these computations. For decays with K^{*+} we combine the results from the two K^* decay channels, by adding their values of $-2 \ln \mathcal{L}$. For the significance S we use the difference between the value of $-2 \ln \mathcal{L}$ for zero signal and the value at its minimum; the corresponding probability is interpreted with the number of degrees of freedom equal to two for modes with a measured f_L and one for the others. For modes without a significant signal, we quote a 90% confidence level (C.L.) upper limit, taken to be the branching fraction below which lies 90% of the total of the likelihood integral in the region of positive branching fraction. In all of these calculations $\mathcal{L}(\mathcal{B})$ is a convolution of the function obtained from the fitter with a Gaussian function representing the correlated and uncorrelated systematic errors detailed below.

We show in Fig. 2 the data and PDFs projected onto m_{ES} . Figure 3 shows similar projections for the $K\pi$ and

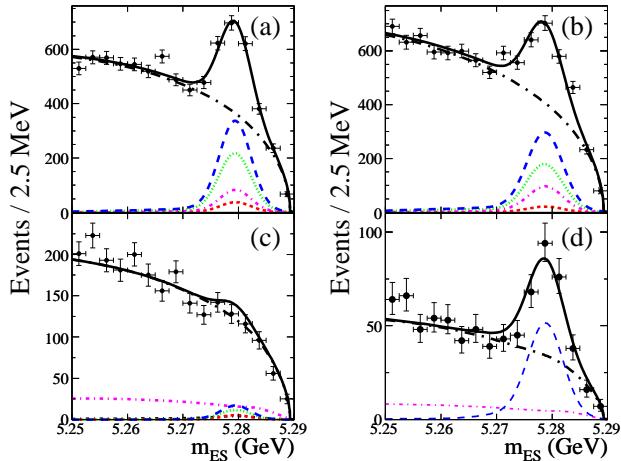


FIG. 2: B -candidate m_{ES} projections for (a) ωK^{*0} , (b) ωK^{*+} , (c) $\omega\rho^0/\omega f_0$, (d) $\omega\rho^+$. The solid curve is the fit function, black long-dash-dotted is the total background, and the blue dashed curve is the total signal contribution. For (a,b) we also show the signal components: $K^*(892)$ (red dashed), $(K\pi)_0^*$ (green dotted), and $K_2^*(1430)$ (magenta dot-dashed). We show for (c,d) the $b \rightarrow c$ background (magenta dot-dashed), and for (c) the $B^0 \rightarrow \omega\rho^0$ (red dashed) and $B^0 \rightarrow \omega f_0$ (green dotted) components. The plots are made with a requirement on $\ln\mathcal{L}$ that has an efficiency of (40-60)% depending on the plot.

$\pi\pi$ masses. Figure 4 gives projections onto \mathcal{H} for the ωK^* modes.

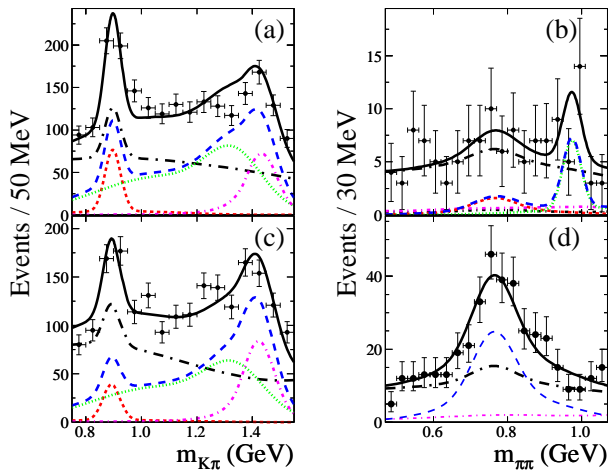


FIG. 3: B -candidate $K\pi$ mass projections for (a) ωK^{*0} , (c) ωK^{*+} , and $\pi\pi$ mass projections for (b) $\omega\rho^0/\omega f_0$, (d) $\omega\rho^+$. The efficiency range and description of the curves are the same as for Fig. 2.

The systematic uncertainties on the branching fractions arising from lack of knowledge of the signal PDF parameters are estimated by varying these parameters within uncertainties obtained from the consistency of fits

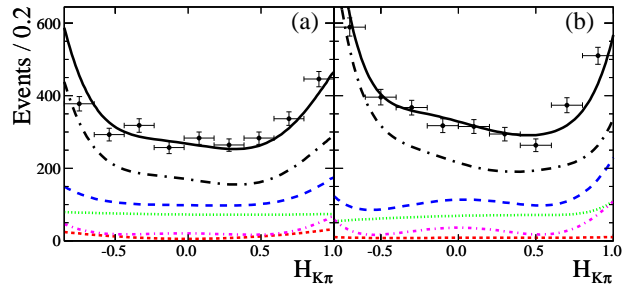


FIG. 4: B -candidate $K\pi$ helicity projections for (a) ωK^{*0} , and (b) ωK^{*+} . The efficiency range and key for the curves are the same as for Fig. 2(a,b).

to MC and data control samples. The uncertainty in the yield bias correction is taken to be the quadratic sum of two terms: half the bias correction and the statistical uncertainty on the bias itself. We estimate the uncertainty from the modeling of the nonresonant and $B\bar{B}$ backgrounds by varying the background yields by their estimated uncertainties (from Ref. [16] and studies of our data). We vary the SXF fraction by its uncertainty; we find this to be 10% of its value, determined from studies of the control samples. For the $K_0^*(1430)$ modes, we vary the LASS parameters within their measured uncertainties [19]. For $B^0 \rightarrow \omega\rho^0$ where f_L is fixed, the uncertainty due to the assumed value of f_L is evaluated as the change in branching fraction when f_L is varied by $^{+0.2}_{-0.3}$. These additive systematic errors are dominant for all modes and are typically similar in size except for the error due to $B\bar{B}$ background, which is usually smaller than the others.

Uncertainties in reconstruction efficiency, found from studies of data control samples, are 0.4%/track, 3.0%/ π^0 , and 1.4%/ K_s^0 decay. We estimate the uncertainty in the number of B mesons to be 1.1%. Published data [16] provide the uncertainties in the B -daughter branching fractions ($\lesssim 2\%$). The uncertainty in the efficiency of the $\cos\theta_T$ requirement is (1.0–1.5)%. Since we do not account for interference among the K^* components, we assign systematic uncertainties based on separate calculations where we vary the phases between the three components over their full range.

The systematic uncertainty on f_L includes the effects of fit bias, PDF-parameter variation, and $B\bar{B}$ and nonresonant backgrounds, all estimated with the same method as used for the yield uncertainties described above. From large inclusive kaon and B -decay samples, we estimate the \mathcal{A}_{ch} bias to be negligible for pions and -0.01 for kaons, due primarily to material interactions. Thus we correct the measured \mathcal{A}_{ch} for the K^* modes by $+0.01$. The systematic uncertainty for \mathcal{A}_{ch} is estimated to be 0.02 due mainly to the uncertainty in this bias correction. This estimate is supported by the fact that the

corrected background \mathcal{A}_{ch} is smaller than 0.015.

In summary, we have searched for nine charmless hadronic B -meson decays as shown in Table II, and have observed most of them (for the first time in all cases except $B^+ \rightarrow \omega\rho^+$). We calculate the branching fractions for $\omega K_0^*(1430)$ using the composition of $(K\pi)_0^*$ from Ref. [20]. We find $\mathcal{B}(B^0 \rightarrow \omega K_0^*(1430)^0) = (16.0 \pm 1.6 \pm 1.5 \pm 2.6) \times 10^{-6}$ and $\mathcal{B}(B^+ \rightarrow \omega K_0^*(1430)^+) = (24.0 \pm 2.6 \pm 2.2 \pm 3.8) \times 10^{-6}$, where the third errors arise from uncertainties in the branching fraction $K_0^*(1430) \rightarrow K\pi$ [16] and the resonant fraction of $(K\pi)_0^*$. For most decays we measure \mathcal{A}_{ch} and find it to be consistent with zero. For VV and VT decays we also measure f_L . For $B^+ \rightarrow \omega\rho^+$, f_L is near 1.0, as it is for $B \rightarrow \rho\rho$ [3]. For the VT $B \rightarrow \omega K_2^*(1430)$ decays f_L is about 4σ from 1.0 for both charge states; it is similar to the value of ~ 0.5 found in $B \rightarrow \phi K^*$ decays. Branching fraction results are in agreement with theoretical estimates [2] except for the SV and VT decays where the estimates are more uncertain [11, 13].

We are grateful for the excellent luminosity and machine conditions provided by our PEP-II colleagues, and for the substantial dedicated effort from the computing organizations that support BABAR. The collaborating institutions wish to thank SLAC for its support and kind hospitality. This work is supported by DOE and NSF (USA), NSERC (Canada), CEA and CNRS-IN2P3 (France), BMBF and DFG (Germany), INFN (Italy), FOM (The Netherlands), NFR (Norway), MES (Russia), MEC (Spain), and STFC (United Kingdom). Individuals have received support from the Marie Curie EIF (European Union) and the A. P. Sloan Foundation.

* Deceased

† Now at Temple University, Philadelphia, Pennsylvania 19122, USA

‡ Now at Tel Aviv University, Tel Aviv, 69978, Israel

§ Also with Università di Perugia, Dipartimento di Fisica, Perugia, Italy

¶ Also with Università di Roma La Sapienza, I-00185 Roma, Italy

** Now at University of South Alabama, Mobile, Alabama 36688, USA

†† Also with Laboratoire de Physique Nucléaire et de Hautes Energies, IN2P3/CNRS, Université Pierre et Marie Curie-Paris6, Université Denis Diderot-Paris7, F-75252 Paris, France

‡‡ Also with Università di Sassari, Sassari, Italy

[1] BABAR Collaboration, B. Aubert *et al.*, Phys. Rev. Lett. **91**, 171802 (2003); Belle Collaboration, K.F. Chen *et al.*, Phys. Rev. Lett. **91**, 201801 (2003).

[2] M. Beneke, J. Rohrer, and D. Yang, Nucl. Phys. B **774**,

64 (2007); H.-Y. Cheng and K.-C. Yang, Phys. Rev. D **78**, 094001 (2008); Y. Li and C.-D. Lü, Phys. Rev. D **73**, 014024 (2006).

[3] Belle Collaboration, A. Somov *et al.*, Phys. Rev. Lett. **96**, 171801 (2006); BABAR Collaboration, B. Aubert *et al.*, Phys. Rev. D **76**, 052007 (2007); Belle Collaboration, J. Zhang *et al.*, Phys. Rev. Lett. **91**, 221801 (2003); BABAR Collaboration, B. Aubert *et al.*, Phys. Rev. Lett. **97**, 261801 (2006).

[4] BABAR Collaboration, B. Aubert *et al.*, Phys. Rev. D **74**, 051102 (2005).

[5] C.W. Bauer *et al.*, Phys. Rev. D **70**, 054015 (2004); P. Colangelo, F. De Fazio, and T.N. Pham, Phys. Lett. B **597**, 291 (2004); A.L. Kagan, Phys. Lett. B **601**, 151 (2004); M. Ladisa *et al.*, Phys. Rev. D **70**, 114025 (2004); H. Y. Cheng, C. K. Chua, and A. Soni, Phys. Rev. D **71**, 014030 (2005); H.-n. Li and S. Mishima, Phys. Rev. D **71**, 054025 (2005); H.-n. Li, Phys. Lett. B **622**, 63 (2005).

[6] A. K. Giri and R. Mohanta, Phys. Rev. D **69**, 014008 (2004); E. Alvarez *et al.*, Phys. Rev. D **70**, 115014 (2004); P. K. Das and K. C. Yang, Phys. Rev. D **71**, 094002 (2005); C.-H. Chen and C.-Q. Geng, Phys. Rev. D **71**, 115004 (2005); Y.-D. Yang, R. M. Wang and G. R. Lu, Phys. Rev. D **72**, 015009 (2005); A. K. Giri and R. Mohanta, Eur. Phys. Jour. C **44**, 249 (2005); S. Baek *et al.*, Phys. Rev. D **72**, 094008 (2005); W. Zou and Z. Xiao, Phys. Rev. D **72**, 094026 (2005); Q. Chang, X.-Q. Li, and Y. D. Yang, JHEP 0706, 038 (2007).

[7] S. Oh, Phys. Rev. D **60**, 034006 (1999).

[8] Belle Collaboration, P. Goldenzweig *et al.*, Phys. Rev. Lett. **101**, 231801 (2008).

[9] D. Atwood and A. Soni, Phys. Rev. D **59**, 013007 (1999); D. Atwood and A. Soni, Phys. Rev. D **65**, 073018 (2002); H.-W. Huang *et al.*, Phys. Rev. D **73**, 014011 (2006).

[10] BABAR Collaboration, B. Aubert *et al.*, Phys. Rev. Lett. **98**, 051801 (2007).

[11] C. S. Kim, J.-P. Lee, and S. Oh, Phys. Rev. D **67**, 014002 (2003).

[12] BABAR Collaboration, B. Aubert *et al.*, Phys. Rev. Lett. **89**, 201802 (2002).

[13] H.-Y. Cheng, C.-K. Chua, and K.-C. Yang, Phys. Rev. D **77**, 014034 (2007).

[14] A. Datta *et al.*, Phys. Rev. D **77**, 114025 (2008).

[15] BABAR Collaboration, B. Aubert *et al.*, Nucl. Instrum. Methods Phys. Res., Sect. A **479**, 1 (2002).

[16] Particle Data Group, C. Amsler *et al.*, Phys. Lett. B **667**, 1 (2008).

[17] BABAR Collaboration, B. Aubert *et al.*, Phys. Rev. Lett. **99**, 171803 (2007).

[18] The BABAR detector Monte Carlo simulation is based on GEANT4: S. Agostinelli *et al.*, Nucl. Instrum. Methods Phys. Res., Sect. A **506**, 250 (2003).

[19] LASS Collaboration, D. Aston *et al.*, Nucl. Phys. B **296**, 493 (1988).

[20] BABAR Collaboration, B. Aubert *et al.*, Phys. Rev. D **72**, 072003 (2005); **74**, 099903(E) (2006).

[21] E791 Collaboration, E. M. Aitala *et al.*, Phys. Rev. Lett. **86**, 765 (2001).